

Geometry of the Orion Bar: Concave or Convex?

William J. Henney¹, Roberto Reyes¹ and Javier García Vázquez¹

¹Universidad Nacional Autónoma de México, Instituto de Radioastronomía y Astrofísica. Antigua Carretera a Pátzcuaro 8701, Ex-Hda. San José de la Huerta, 58089, Morelia, Michoacán, México

Keywords: keyword 1, keyword 2, keyword 3, keyword 4, keyword 5

Abstract

I critically examen different geometrical models that have been proposed for the geometry of the Orion Bar photodissociation region. From a re-analysis of the of the 21 cm H I observations, I show that the ionization front at the Bar must be convex, which rules out important classes of models. On the other hand, from the brightness profiles of recombination lines and continuum, I show that maybe it is convex after all. Furthermore, I show that small scale irregularities in the ionization front and dissociation front are important for analysing the apparent stratification and widths of different emission regions.

Resumen

Resumen en español.

Corresponding author: William J. Henney *E-mail address:* w.henney@irya.unam.mx

Received: April 16th, 2024 **Accepted:** November 6, 2025

1. INTRODUCTION

Welcome to the RMxAA L^AT_EXtemplate to prepare your academic article. Articles considered for publication in the main journal can be easily prepared using this template. The style of this template is based on the *rho class* style¹. It requires minimal or no typesetting adjustments to provide a version of your manuscript organization that is close to the final printed version. This style also has ample margins to allow for a comfortable number of words per line and leaves room for marginal notes to be added.

The version of the rmaa-rho document class described in this User Guide is 1.0 (November 6, 2025). Its use requires a relatively recent version of L^AT_EX, although it is optimized to work directly online using Overleaf. The current version of the L^AT_EX Project Public License is 1.3c (2008). For the author who requires a general introduction to L^AT_EX, we recommend starting at The LaTeX Project website <https://www.latex-project.org/about/>, or using the Overleaf LaTeX guide [https://www.overleaf.com/learn/latex/Free_online_introduction_to_LaTeX_\(part_1\).](https://www.overleaf.com/learn/latex/Free_online_introduction_to_LaTeX_(part_1).)

2. STRUCTURE OF THE ORION BAR

2.1. Cloudy model predictions for the optical depths

In order to investigate the role of dust extinction in greater detail in more detail the

Location of H⁰. Neutral veil in front of nebula has column density of $1.6 \times 10^{21} \text{ cm}^{-2}$ and $3.2 \times 10^{21} \text{ cm}^{-2}$ in components A and B (Abel et al., 2006).

Geometry of bar: in Henney et al. (2005) I pointed out that a diverging cylindrical geometry is necessary to explain the sharp peak in the [N II] emissivity seen at the ionization front. It has been apparent since O'Dell & Yusef-Zadeh (2000) that the nebula contains many bar-like features.

Salgado et al. (2016) had found low dust cross-section in Orion Bar PDR, but there are loopholes. First, they assume plane-parallel geometry with exactly edge-on viewing angle, while in reality it is a roughly cylindrical filament. Second, they ignore scattering, see Watson et al. (1998). Also, density increase with depth

3. MODEL BRIGHTNESS PROFILES

Present the horn profiles and show the difference between the convex and concave case. Homogeneous layer, or more refined models for ionized flow and PDR.

4. H I 21 cm RADIATIVE TRANSFER

Karl G. Jansky Very Large Array observations of the H I 21 cm line from the Orion Nebula and its surroundings at a spatial resolution of $\approx 6''$ and a velocity resolution of 0.77 km s^{-1} were presented in van der Werf et al. (2013, hereafter vdW13). The line is seen both in emission and absorption of the strong free-free continuum emitted by the ionized nebula. The majority of the absorption arises in the foreground Veil at Local Standard of Rest velocities of $v_{\text{lsr}} = -2 \text{ km s}^{-1}$ to $+7 \text{ km s}^{-1}$. Emission is seen primarily at more redshifted velocities of $+10 \text{ km s}^{-1}$ to $+15 \text{ km s}^{-1}$, similar to the velocities of the molecular gas seen in CO, although at large distances from the center of the nebula the Veil is also seen in emission. The analysis of the absorption components by vdW13

¹The RMxAA paper template is based on the rho LATEX class, created by Luis Guillermo Jiménez López and Eduardo Gracidas Reyes.

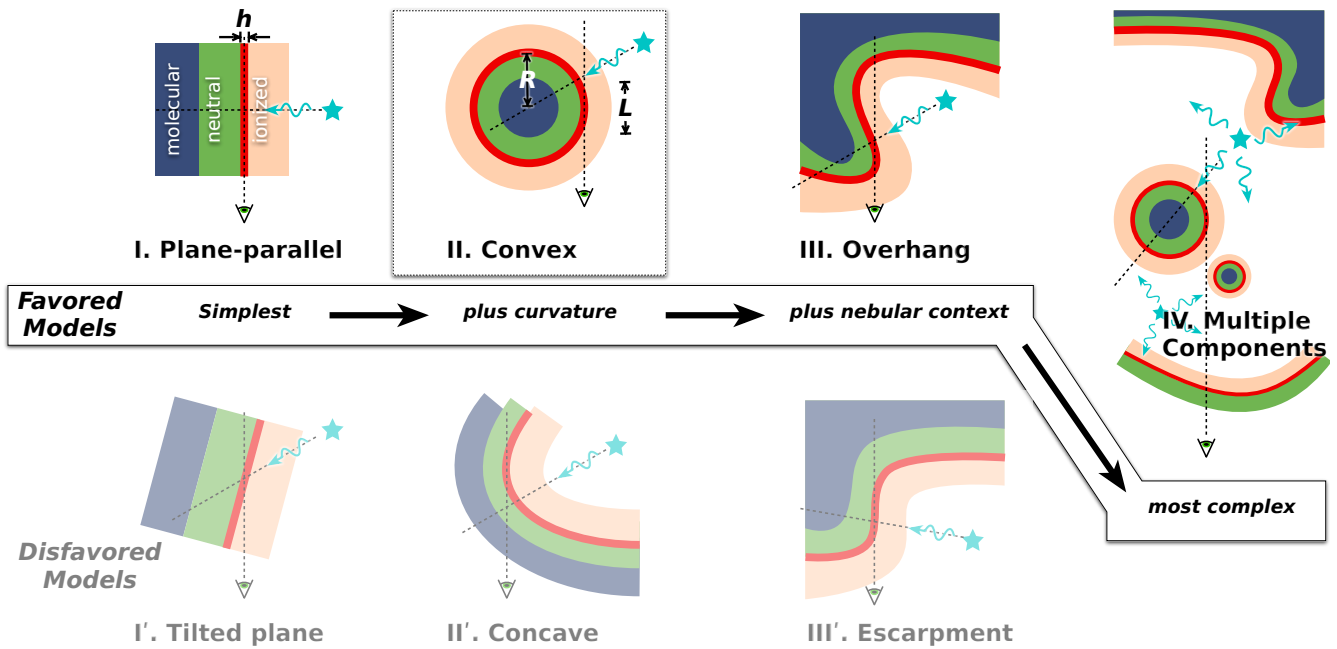


Figure 1. Different classes of geometrical models that have been proposed for the Orion Bar. The sequence of models I, II, III, IV are of increasing complexity, but also increasing scope and explanatory power. Models I', II', III', on the other hand, are disfavored due to either underperformance or falsification (see text for further details). For all models, dark blue shading represents molecular gas, green shading represents neutral gas, and light orange shading represents ionized gas. An example emission layer of thickness h and radius of curvature R is indicated by thick red lines. The line-of-sight depth of the emission layer is denoted by L . The direction of illumination and the line of sight are indicated by thin dotted lines.

55 was carried out under the assumptions that (i) all of the continuum
 56 emission arises from *behind* the absorbing H⁰ column (from the
 57 point of view of the Earth), and (ii) line emission is negligible
 58 at velocities where absorption is detected. These are both very
 59 good assumptions in the case of absorption by the foreground
 60 Veil, but they break down for the case of the Orion Bar, where
 61 both emission and absorption are seen at similar velocities and
 62 in spatially adjacent regions. Given the wealth of information on
 63 the physical conditions and geometry that these data provide, it
 64 is worth reanalyzing them under less restrictive assumptions.

65 In the Rayleigh-Jeans limit, the frequency-dependent surface
 66 brightness I_ν is characterized by the brightness temperature in
 67 each velocity channel: $T_b(v) = c^2 I_\nu / 2k\nu^2$, where $v/c = (\nu/\nu_0) - 1$
 68 and $\nu_0 = 1.420\,405$ GHz. The radiative transfer equation can
 69 be solved for an idealized three-layer sandwich structure (see
 70 Fig. 4), consisting of (1) a background H⁺ region with electron
 71 temperature T_e and free-free continuum optical depth τ' , (2) an
 72 intermediate neutral H⁰ layer with spin temperature T_s and line
 73 optical depth $\tau(v)$, and (3) a foreground H⁺ region with the
 74 electron temperature T_e and free-free continuum optical depth
 75 τ'' . The continuum source function in regions 1 and 3 is T_e ,
 76 whereas the line source function in region 2 is T_s . Region 2 is
 77 assumed to have zero continuum optical depth. Following vdW13,
 78 large-scale Milky Way H I line emission along the line of sight
 79 through Orion is neglected since it is (a) very faint compared with
 80 the nebula, with $T_b(v) < 48$ K at $v = 10$ km s⁻¹ (Green, 1991;
 81 Green & Padman, 1993), and (b) any emission that is smooth
 82 on angular scales below 7 arcminutes will be filtered out by the
 83 interferometer.

84 At continuum frequencies just off the line, $\tau(v) = 0$ and only
 85 regions 1 and 3 contribute to the observed brightness, yielding a

continuum brightness temperature

$$\begin{aligned} T_c &= T_e \left(1 - e^{-(\tau' + \tau'')} \right) \\ &= T_e' e^{-\tau''} + T_e'', \end{aligned} \quad (1)$$

where the second equality gives the decomposition into separate
 87 contributions from region 1: $T_e' = T_e(1 - e^{-\tau'})$, and region 3:
 88 $T_e'' = T_e(1 - e^{-\tau''})$. At frequencies where the line opacity is
 89 significant, all three regions contribute, yielding
 90

$$T_b(v) = T_e' e^{-(\tau(v) + \tau'')} + T_s \left(1 - e^{-\tau(v)} \right) e^{-\tau''} + T_e''. \quad (2)$$

For practical reasons related to the deconvolution of the
 91 interferometric data, the results of vdW13 are presented in
 92 continuum-free form as $\tilde{T}_b(v) = T_b(v) - T_c$. Combining
 93 equation (1) and (2), one finds
 94

$$\tilde{T}_b(v) = [1 - e^{-\tau(v)}] [1 - (T_e''/T_e)] [T_s - T_e']. \quad (3)$$

The relative brightness temperature of the line, $\tilde{T}_b(v)$, is therefore
 95 seen to be the product of three factors, given by the three sets of
 96 square brackets in equation (3). The first two factors are always
 97 positive since $\tau(v) \geq 0$ and $T_e'' \leq T_e$, but the third factor can
 98 take either sign. When the continuum brightness temperature T_e'
 99 of the background photoionized gas in region 1 exceeds the spin
 100 temperature T_s of neutral hydrogen in region 2, then we see an
 101 absorption line: $\tilde{T}_b(v) < 0$. On the other hand, when T_s is higher
 102 than T_e' , then we see an emission line: $\tilde{T}_b(v) > 0$. In either
 103 case, the maximum line strength will be found when region 2
 104 is opaque ($\tau(v) \gg 1$) and region 3 is transparent ($T_e'' \ll T_e$),
 105 yielding $\max(|\tilde{T}_b(v)|) = |T_s - T_e'|$.

The electron temperature in the ionized gas is expected to be

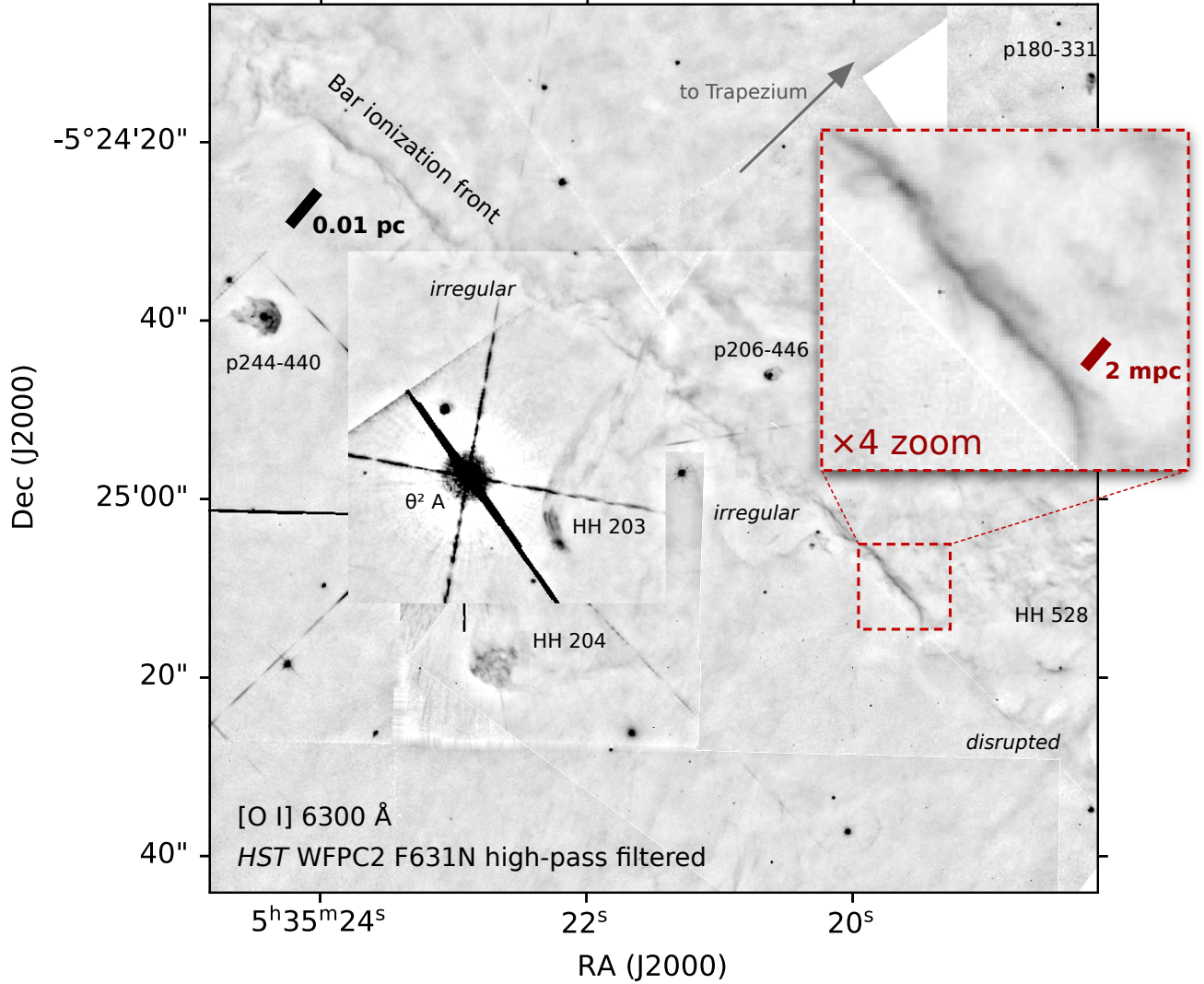


Figure 2. Fine-scale structure of the ionization front at the Orion Bar. Grayscale image shows a $90'' \times 90''$ section of a mosaic of *HST* WFPC2 observations (Bally et al., 2000) in the F631N filter, which mainly passes the [O I] 6300 Å line. The image has been high-pass filtered to remove large-scale brightness gradients (> 16 arcsec). The principal ionization front of the Bright Bar runs diagonally from top-left to bottom-right. It can be seen that the front is very irregular on scales of 1 to 10 mpc, and even becomes disrupted completely in some segments. Only in a few places is the front straight and regular enough for its true sharpness to be seen, such as the small area shown in a zoomed box, where the width of the [O I] ridge can be seen to be less than 1 mpc. Apart from the Bright Bar ionization front, other fine-scale features visible in the image are associated with Herbig–Haro jets and proplyds.

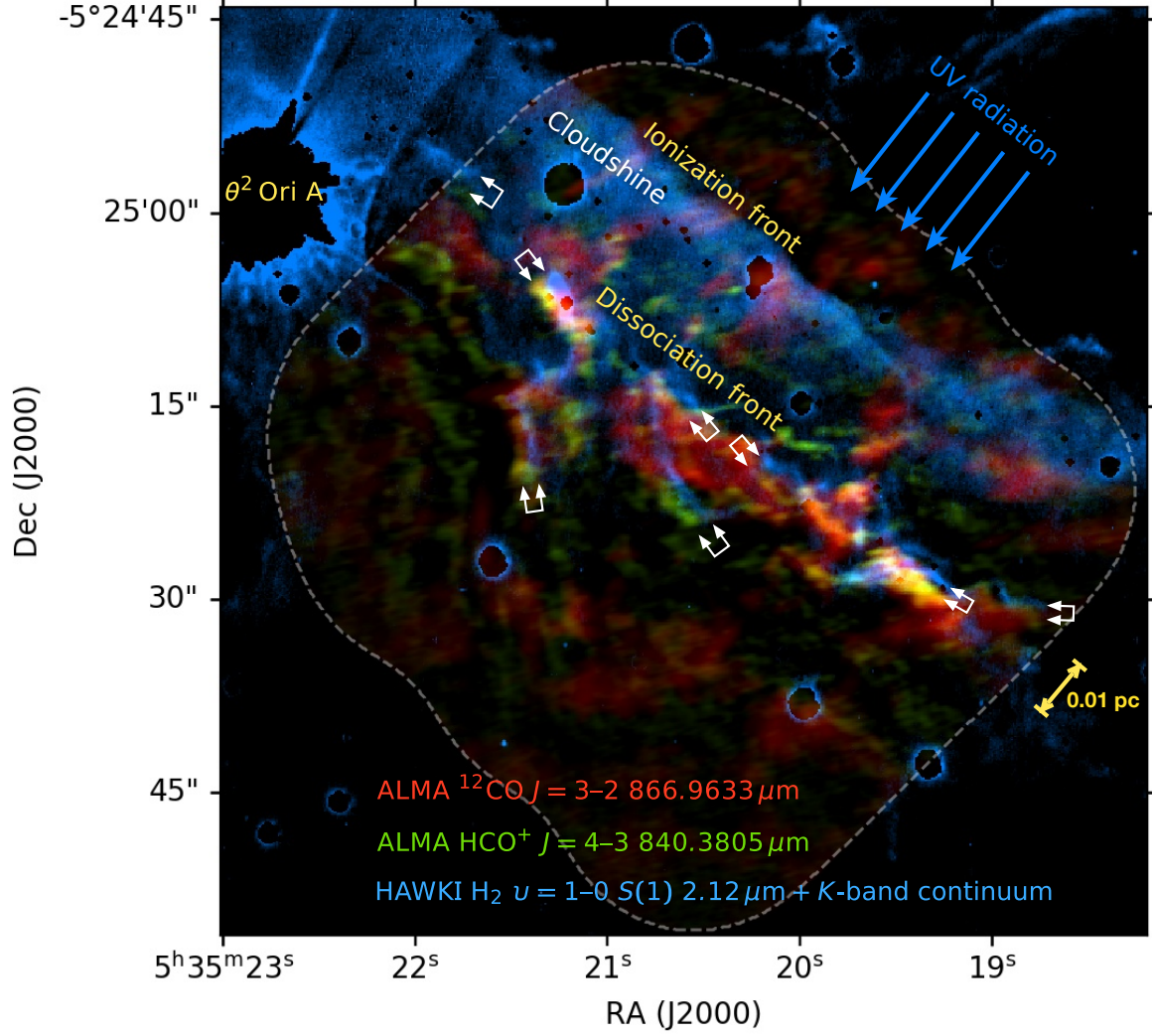


Figure 3. Fine-scale structure of the dissociation front in the Orion Bar. Double white arrows mark out some instances of stratification between emission of H₂ (blue) and heavier molecules (green/yellow/red). In every instance H₂ is displaced towards the irradiated side of the filament by 1'' to 2'' (≈ 0.003 pc). Background image shows ALMA mosaics (Goicoechea et al., 2016) of the sub-mm CO $J = 3 \rightarrow 2$ 866.96 μm HCO⁺ 840.38 μm emission lines in the red and green color channels, respectively, with the boundary of the ALMA field shown by the gray dashed line. The blue color channel of the background image shows near-infrared vibrationally excited H₂ $\nu = 1 \rightarrow 0$ S(1) 2.12 μm emission, extracted from narrow-band imaging with ESO's High Acuity Wide-field K-band Imager (HAWK-I, Kissler-Patig et al., 2008). The H₂ image has been corrected for contamination by ionized emission (mainly hydrogen Brγ recombination line), but has not been continuum-subtracted. As a result, scattered starlight (cloudshine, Foster & Goodman, 2006) is seen as a band of diffuse emission that falls off smoothly behind the ionization front.

Figure 4. Three-layer sandwich structure for H I 21 cm radiative transfer.

roughly constant at $T_e \approx 11\,000$ K (Dicker et al., 2009), but this still leaves 4 unknown quantities, $\tau(v)$, T_s , T_c' , and T_c'' , to be determined from 2 observed quantities: T_c and $\tilde{T}_b(v)$. Further assumptions must therefore be made in order to interpret the observations, but these can be guided by the observed spatial trends and simple geometric models. For instance, in the Orion Bar the free-free continuum brightness temperature falls sharply across the ionization front from $T_c \approx 3000$ K on the ionized side, but then levels off to a roughly constant value of $T_c \approx 600$ K on the neutral side. Assuming that this constant value reflects unrelated foreground emission (probably ionized by θ^2 Ori A) that overlays the entire Bar (this hypothesis is tested below), we have an upper limit to the background emission of $T_c - 600$ K. It can be further assumed that the emission from region 1 is a constant fraction, f_{bg} , of this upper limit:

$$T_c' = f_{bg}(T_c - 600 \text{ K}). \quad (4)$$

If the Bar geometry is a cylinder that is illuminated from the side (see Fig. XXX), then $f_{bg} = 0.5$ is appropriate. If the Bar is illuminated from slightly behind, or if it is an escarpment, or if an additional background component is present (see § 2), then the fraction will be larger: $0.5 < f_{bg} < 1.0$.

Further progress can then be made by considering null points in the nebula where line emission and absorption cancel out. At such points $\tilde{T}_b(v) \approx 0$, so that $T_s = T_c'$ by equation (3). Absorption component M is identified by vdW13 as associated with H^0 in the Bar, due to its velocity and spatial distribution. Component M consists of a string of knots with $\tilde{T}_b(v) = -200$ to -400 K at $v \approx 11 \text{ km s}^{-1}$. They are arranged parallel to the Bar, just behind the ionization front at a relative position of roughly $+0.006$ pc (see Fig. ??) and where the continuum brightness has fallen to $T_c \approx 2200$ K. At greater distances from the ionization front the H I at this velocity is seen in emission, reaching a peak of $\tilde{T}_b(v) \approx +250$ K at $+0.030$ pc where $T_c \approx 750$ K. The crossover null point where $\tilde{T}_b(v) = 0$ occurs between these two at $+0.012$ pc where $T_c \approx 1500$ K.

5. CONCEPT HIGHLIGHT BOX

The new RMxAA L^AT_EX macro allows the authors to use a colored box to highlight a concept or equation, as shown in this example. The label and reference points of the section are included. Example: See the Concept box in Section 5.

Highlight Concept Box

Hello! This is an example of a concept highlight box (HCB) section. I can be placed anywhere in the body of the paper to briefly summarize the important concepts. We do not allow HCBs larger than 40 words

6. FACILITIES

For observational research, authors must include a brief list of facilities and instruments used, as well as proper acknowledgment of public catalogs and virtual observatory resources.

■ REFERENCES

- | | |
|--|-----|
| Abel, N. P., Ferland, G. J., O'Dell, C. R., Shaw, G., & Troland, T. H. | 151 |
| 2006, ApJ, 644, 344, doi: 10.1086/500819 | 152 |
| Bally, J., O'Dell, C. R., & McCaughrean, M. J. 2000, AJ, 119, 2919, | 153 |
| doi: 10.1086/301385 | 154 |
| Dicker, S. R., Mason, B. S., Korngut, P. M., et al. 2009, ApJ, 705, | 155 |
| 226, doi: 10.1088/0004-637X/705/1/226 | 156 |
| Foster, J. B., & Goodman, A. A. 2006, ApJ, 636, L105, doi: 10.1086/500131 | 157 |
| Goicoechea, J. R., Pety, J., Cuadrado, S., et al. 2016, Nature, 537, | 158 |
| 207, doi: 10.1038/nature18957 | 159 |
| Green, D. A. 1991, MNRAS, 253, 350, doi: 10.1093/mnras/253.2.350 | 160 |
| Green, D. A., & Padman, R. 1993, MNRAS, 263, 535, doi: 10.1093/mnras/263.2.535 | 161 |
| Henney, W. J., Arthur, S. J., Williams, R. J. R., & Ferland, G. J. | 162 |
| 2005, ApJ, 621, 328, doi: 10.1086/427491 | 163 |
| Kissler-Patig, M., Pirard, J. F., Casali, M., et al. 2008, A&A, 491, | 164 |
| 941, doi: 10.1051/0004-6361:200809910 | 165 |
| O'Dell, C. R., & Yusef-Zadeh, F. 2000, AJ, 120, 382, doi: 10.1086/301429 | 166 |
| Salgado, F., Berné, O., Adams, J. D., et al. 2016, ApJ, 830, 118, | 167 |
| doi: 10.3847/0004-637X/830/2/118 | 168 |
| van der Werf, P. P., Goss, W. M., & O'Dell, C. R. 2013, ApJ, 762, | 169 |
| 101, doi: 10.1088/0004-637X/762/2/101 | 170 |
| Watson, A. M., Henney, W. J., & Escalante, V. 1998, in American | 171 |
| Astronomical Society Meeting Abstracts, Vol. 193, 16.03 | 172 |

7. ACKNOWLEDGEMENTS

Acknowledgements may be included to recognize funding sources and grants, to provide standardized acknowledgement text (including required references) for facilities or resources, and/or to recognize individuals who contributed to the research with any relevant discussion, resources, or services but are not listed as coauthors.

8. APPENDICES

If you have appendices to your article, you can use something like the following:

```
\begin{appendices}
\section{First Appendix}
\label{sec:ap-A}
\{Text of first appendix.\}
\section{Second Appendix}
\label{sec:ap-B}
\{Text of second appendix.\}
\end{appendices}
```

The appendices follow the acknowledgments section but precede the bibliography section. Equations in the appendices are labeled A1, A2, B1, B2, etc..

9. CODES

This macro includes the *listings* package, which offers customized features for adding codes or pseudocodes. The package adds adequate syntax coloring for some of the most popular languages (C, C++, Python, and Matlab).

```

1 function fibonacci_sequence(num_terms)
2     % Initialize the first two terms of the sequence
3     fib_sequence = [0, 1];
4
5     if num_terms < 1
6         disp('Number of terms should be greater than
7             or equal to 1.');
7         return;
8     elseif num_terms == 1
9         fprintf('Fibonacci Sequence:\n%d\n',
10            fib_sequence(1));
11         return;
12     elseif num_terms == 2
13         fprintf('Fibonacci Sequence:\n%d\n%d\n',
14            fib_sequence(1), fib_sequence(2));
15         return;
16     end
17
18     % Calculate and display the Fibonacci sequence
19     for i = 3:num_terms
20         fib_sequence(i) = fib_sequence(i-1) +
21             fib_sequence(i-2);
22     end
23
24     fprintf('Fibonacci Sequence:\n');
25     disp(fib_sequence);
26 end

```

207
208
209
210
211

enabled to facilitate referee revision. We recommend placing the command \nolinenumbers at the beginning and \linenumbers at the end of the code, respectively. This temporarily removes the line numbering for the manuscript and provides code line numbers.

Code 1. Example of matlab code.

```

1 import numpy as np
2 import matplotlib.pyplot as plt
3 from scipy.optimize import curve_fit
4
5 def linear_model(x, m, b):
6     return m * x + b
7
8 def fit_regression(x, y, ex, ey):
9     # Ajuste ponderado por errores en y
10    popt, pcov = curve_fit(linear_model, x, y, sigma=
11        ey, absolute_sigma=True)
12    m_opt, b_opt = popt
13    perr = np.sqrt(np.diag(pcov))
14    m_err = perr[0] # Incertidumbre en la pendiente
15    return m_opt, b_opt, m_err
16
17 def plot_regression(x, y, ex, ey, m_opt, b_opt, m_err):
18
19    plt.errorbar(x, y, xerr=ex, yerr=ey, fmt='o',
20        label='Datos', ecolor='gray', capsize=3)

```

Code 2. Example of Python code.

```

1 Pseudo Code:
2 Read isfive
3 If(isfive = 5)
4     Write "your number is 5"
5 Else if (isfive = 6)
6     Write "your number is 6"
7 Else
8     Write "your number is not 5 or 6"

```

Code 3. Example of Pseudo-code.

206 During the paper edition process, line numbering will be